# Capillary behaviors of miscible fluids in porous media: a pore-scale simulation study

Ronghao Cui[0000−0002−4590−4666] and Shuyu Sun(✉)[0000−0002−3078−864X]

Computational Transport Phenomena Laboratory (CTPL), Physical Science and Engineering (PSE) Division, King Abdullah University of Science and Technology (KAUST), Thuwal 23955-6900, Saudi Arabia
shuyu.sun@kaust.edu.sa

**Abstract.** Capillary behaviors of two phases in porous media are widely investigated by pore-scale simulations. Flow properties of miscible two-phase fluids pose challenges because compositional species in miscible fluids exist in both of two phases. In this work, pore-network modeling is developed to analyze capillary behaviors of miscible fluids. First, the pore-network structure is generated by introducing the Halton sequence and the Delaunay triangulation. Then, we perform the primary drainage to simulate the variation of capillary pressure as a function of saturation under equilibrium conditions. The miscibility details of two-phase fluids are determined by two-phase flash calculations. The effect of representative network sizes on capillary behaviors is analyzed to balance computational demands and interpretability. Our models demonstrate the efficiency and the robustness of the network generation procedure. Finally, our simulation results indicate that the miscibility of fluids significantly influences capillary behaviors, highlighting the necessity of species-specific compositional modeling for miscible two-phase fluids in porous media.

**Keywords:** Pore-scale simulation · Capillary pressure · Miscible fluids.

## 1 Introduction

Two-phase flow of fluids in subsurface porous media has been playing an important role in energy resources exploitation and carbon geological storage. Compared with gas-water or oil-water two phases that have been traditionally modeled as immiscible phases, gas-oil two phases can be miscible and then simulated by species-specified compositional flow [1, 2]. Species in miscible fluids can exist in both of two phases, leading to complex phase and interfacial behaviors. These behaviors are heavily affected by temperature, pressure, and composition conditions. Understanding the flow properties of miscible phases is one of the key issues to enhance sustainable recovery of hydrocarbon resources and stable storage of greenhouse gases.

Capillary pressure $p_c$ plays an essential role in residual trapping of fluids during the two-phase flow in porous media. The variation of $p_c$ as a function of

ICCS Camera Ready Version 2024
To cite this paper please use the final published version:
DOI: 10.1007/978-3-031-63783-4_1

the wetting-phase saturation $S_w$ is known as the $p_c$-$S_w$ curve. In fact, the $p_c$-$S_w$ curve is one of the most common constitutive properties of two-phase flow in porous media. The $p_c$-$S_w$ curve can be obtained from laboratory experiments and numerical simulations. Compared with laboratory experiments, numerical simulations overcome the limitations at spatial and temporal scales to investigate the $p_c$-$S_w$ curve in porous media under equilibrium conditions [3]. The prevalent numerical method for the $p_c$-$S_w$ curve is pore-network modeling with the low computational cost. A pore-network model is composed of pore bodies and pore throats with simple geometries. Pore bodies mainly contribute to network saturations and serve as computational nodes for flow simulations [4]. The miscible two-phase fluids involve the equation of state (EoS) to characterize their physical properties. As one of the most prevalent EoSs, the Peng-Robinson EoS has shown excellent estimation for hydrocarbon phase behaviors. Two-phase flash calculations are the important part of phase equilibrium calculations to obtain details of compositional species in each phase. Successive substitution iteration and Newton's method are popular methods to solve the formulations of two-phase flash problems [5].

The workflow of this work is summarized as follows. We at first introduce the Halton sequence and Delaunay triangulation in the pore-network generator to create the pore-network structure. Then, we perform the primary drainage simulations to compute $p_c$-$S_w$ curves. We evaluate the effect of representative network sizes based on the outcomes of $p_c$-$S_w$ curves in order to optimize the computational cost and interpretability. At last, we consider binary miscible fluids whose two-phase information is obtained from flash calculations to investigate the capillary behaviors in porous media.

## 2 Methodology

### 2.1 The network structure

In this work, we have developed random generator-based pore-network models for flow simulations. The generation procedure is summarized as follows. At first, the network topology was determined by creating a given number of pore bodies distributed in a two-dimensional (2D) square domain. We generated quasirandom pore bodies in this 2D space by use of the Halton sequence. Compared with the source of pseudorandom numbers, pore bodies created by the Halton sequence is of lower discrepancy in distribution but not uniformly cover the domain [6]. Second, we connected pore bodies by pore throats using the Delaunay triangulation method to create triangles in the 2D domain [7]. In practice, we predefined a specific number of pore bodies based on the density of pore bodies within the 2D domain, positioning them at the four domain boundaries to avoid lengthy pore throats. For approximating the statistical properties of the porous media, pore throats between pore bodies were randomly deleted according to the averaged coordination number. The pore-throat deletion was followed by the elimination process which was conducted to delete isolated pore bodies, isolated clusters, and dead-end pore bodies by use of the method proposed by Raoof

ICCS Camera Ready Version 2024
To cite this paper please use the final published version:
DOI: 10.1007/978-3-031-63783-4_1

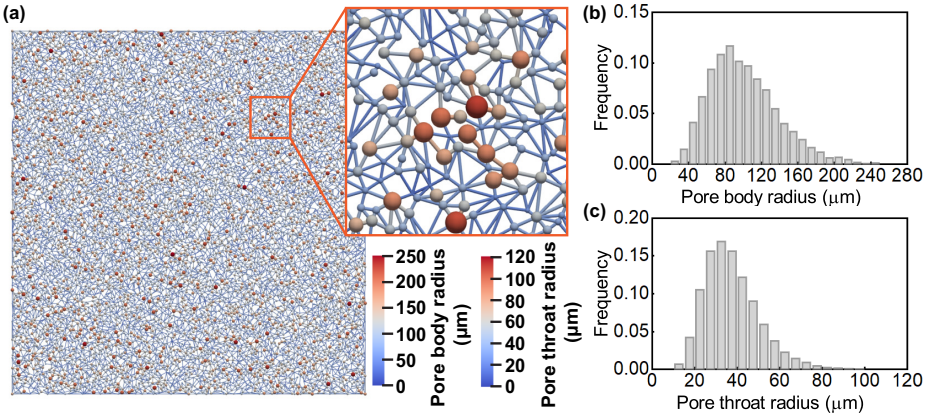


**Fig. 1.** The pore-network model consisting of 10050 pore bodies and 25094 pore throats with the average coordination number of 5.0: (a) the structure illustration, (b) the inscribed radius distribution of pore bodies, and (c) the inscribed radius distribution of pore throats.

and Hassanizadeh [8]. Third, we determined pore body sizes by the lognormal distribution function, while pore throat sizes were assigned according to their neighboring pore bodies at both ends [9, 10]. We used cube as the geometry of pore bodies and square as the cross-sectional shape of pore throats. These angular geometries can accommodate two phases simultaneously. An example of the pore-network model we generated is shown in Fig. 1a. In this case, we generated 10050 pore bodies and 25094 pore throats with the average coordination number of 5.0. Figs. 1b and 1c show the generated inscribed radius distributions of pore bodies and pore throats, respectively.

### 2.2 Numerical experiments

Miscible fluids we used in this work can be partitioned into two phases, vapor and liquid. We simulated the primary vapor drainage in a strongly liquid-wet porous medium to obtain $p_c$-$S_w$ curves, where contact angle was assumed as zero. Therefore, we did not consider the effect of contact angles on capillary pressure. The primary drainage process can be explained as follows. The liquid phase is initially saturated in the pore network at the given temperature and pressure. The vapor phase starts to contact the pore network at the same temperature. With the increase of the vapor phase, there is a gradual increment of capillary pressure between two phases in the pore network. At each step of capillary pressure, equilibrium positions of all gas-liquid interfaces within the network are determined. Then, computations are carried out for wetting-phase saturation $S_w$ within the entire pore network. As a results, a $p_c$-$S_w$ curve for the network can be obtained.

ICCS Camera Ready Version 2024
To cite this paper please use the final published version:
DOI: 10.1007/978-3-031-63783-4_1

Non-wetting phase invasion in pore throats is controlled by entry capillary pressure formulated by the MS-P theory involving interfacial tension $\sigma$, pore throat radius $r_t$, contact angle $\theta$ [11]. Due to the assumption of $\theta$=0° in this work, the entry capillary pressure is dependent on $\sigma$ with the given $r_t$. We have calculated $\sigma$ for miscible fluids which have $N_c$ components using the Weinaug-Katz equation:

$$\sigma = \big[\sum_{j=1}^{N_c}(\chi_j x_j c_w - \chi_j y_j c_n)\big]^E \tag{1}$$

where $\chi_j$ is the parachor of component $j$, $x_j$ and $y_j$ are mole fractions of component $j$ in liquid and vapor phases, respectively, $c_w$ and $c_n$ are molar densities of liquid and vapor phases, respectively, and $E$ is the critical scaling exponent ($E = 4.0$). The parachor is an empirical value for the given component species [12]. For calculating $\sigma$, we need to know the compositional variables of two phases, including $x_j$, $y_j$, $c_w$, $c_n$. Two-phase flash calculations can be used to compute these compositional variables. With the known overall composition $z_j$ for miscible fluids, the fugacities of each species in liquid and vapor phases, $f_j^L$ and $f_j^V$, are supposed to be equal to each other, i.e., $f_j^L$=$f_j^V$. Knowing liquid and vapor pressures, $p^L$ and $p^V$, we have introduced corresponding fugacity coefficients, $\varphi_j^L$ and $\varphi_j^V$, where $f_j^L = \varphi_j^L x_j p^L$ and $f_j^V = \varphi_j^V y_j p^V$. The vapor-liquid equilibrium ratio for component $j$, $K_j$, is defined as the ratio of $y_j$ to $x_j$ ($K_j = y_j/x_j$). Based on the fugacity equivalence relation, $K_j$ is computed as given by:

$$K_j = \frac{\varphi_j^L p^L}{\varphi_j^V p^V} \tag{2}$$

EoSs play an important role in two-phase flash calculations, since $\varphi_j^L$ and $\varphi_j^V$ are calculated from EoSs [5]. In this work, we have employed the Peng-Robinson EoS for miscible fluids. The vapor-phase mole fraction in miscible fluids is defined as $\beta^V = N^V/N$, where $N^V$ and $N$ are mole numbers of the vapor phase and overall miscible fluids, respectively. With $\beta^V$, $K_j$, and $z_j$, the Rachford-Rice equation ($F_{RR} = 0$) is given by:

$$F_{RR} = \sum_{j=1}^{N_c} \frac{(K_j - 1)z_j}{1 + \beta^V(K_j - 1)} = 0 \tag{3}$$

Two-phase flash formulations are solved by successive substitution iteration in this work. Without any information about vapor-liquid two-phase equilibrium to calculate $K_j$ from Eq. 2 at the beginning of two-phase flash calculations, Wilson's correlation with thermodynamic properties of fluids is employed to obtain the initial guess of $K_j$, as given by:

$$K_j^0 = \frac{p_{c,j}}{p^V} \exp(5.37(1 + \omega_j)(1 - \frac{T_{c,j}}{T})) \tag{4}$$

where $\omega_j$ is the acentric factor of component $j$, $T_{c,j}$ and $p_{c,j}$ are critical temperature and critical pressure of component $j$, respectively, and $T$ is the temperature.

ICCS Camera Ready Version 2024
To cite this paper please use the final published version:
DOI: 10.1007/978-3-031-63783-4_1

With known $K_j$ ($K_j = K_j^0$ for the first step), the Rachford-Rice equation (Eq. 3) is solved to obtain $\beta^V$. Next, the Peng-Robinson EoS is employed to get $\varphi_j^L$ and $\varphi_j^V$ for updating $K_j$ according to Eq. 2. Related EoS parameters used in this work can be found in Ref. [12]. Successive substitution iteration repeats updating $K_j$ and $\beta^V$ until the convergence is reached.

## 3 Results and discussion

### 3.1 The representative network size

The representative elementary volume (REV) size is an important issue when investigating flow properties in porous media. The REV effect is analyzed using our pore-network model to obtain the representative network size. As shown in Fig. 2, we selected 400, 2000, and 4000 pore bodies generated within the square domain. The interfacial tension is set as 72.8mN/m. We performed the primary vapor drainage and calculated $p_c$-$S_w$ curves in pore-network models for 20 runs using the same input parameters. It can be seen that the network sizes heavily influence $p_c$-$S_w$ curves during the drainage. With 400 pore bodies, there are large variations of $p_c$-$S_w$ curves for different runs. As the number of pore bodies increases, $p_c$-$S_w$ curves from each run gradually approaches the average curve. Fig. 2 shows that $p_c$-$S_w$ curves are not significantly influenced by the network size when containing 4000 pore bodies. Therefore, we used 4000 pore bodies to simulate the drainage process for miscible fluids. It should be noted that this is only valid for our 2D models. If there is a three-dimensional (3D) pore-network model, the best representative network size will change. This is because 3D pore-network models can have higher coordination number for pore bodies than the 2D version.

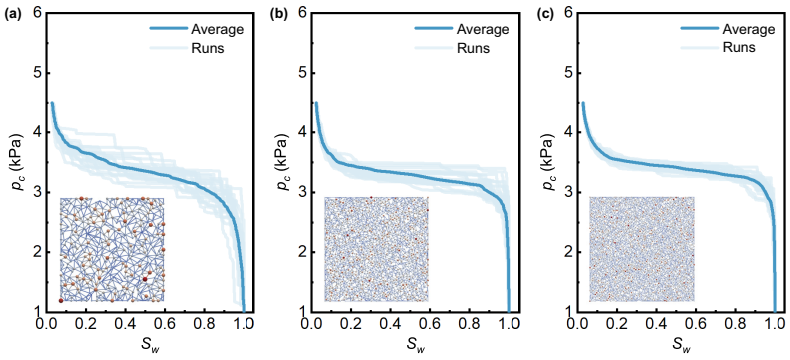


**Fig. 2.** The effect of representative network sizes on $p_c$-$S_w$ curves: (a) 400 pore bodies, (b) 2000 pore bodies, and (c) 4000 pore bodies.

ICCS Camera Ready Version 2024
To cite this paper please use the final published version:
DOI: 10.1007/978-3-031-63783-4_1

### 3.2 Capillary behaviors of miscible fluids

To investigate capillary behavoirs of different miscible fluids in porous media, we consider binary mixtures consisting of one component selected from nitrogen($N_2$), methane($C_1$), or carbon dioxide ($CO_2$), and the other one chosen from n-butane ($nC_4$), n-pentane ($nC_5$), or n-decane ($nC_{10}$). It should be noted that we have performed the primary vapor drainage only when there exist two phases. As a matter of fact, one single phase for miscible fluids may occur under appropriate temperature and pressure conditions. Due to the monotonically decreasing function of $\beta^V$ in the Rachford-Rice equation ($F_{RR}$ in Eq. 3), we roughly used the values of $F_{RR}|_{\beta=0}$ and $F_{RR}|_{\beta=1}$ to determine whether there were two phases. In the case of two phases, it is required that $F_{RR}|_{\beta=0}>0$ and $F_{RR}|_{\beta=1}<0$. However, a more rigorous examination of phase states should utilize the procedure of phase stability analysis [5].

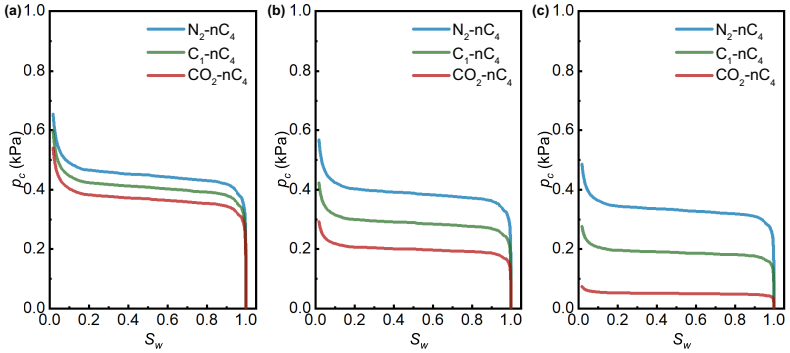


**Fig. 3.** The capillary behaviors of $N_2$-$nC_4$, $C_1$-$nC_4$, and $CO_2$-$nC_4$ miscible fluids at $T$=323K: (a) $p^V$=2MPa, (b) $p^V$=4MPa, and (c) $p^V$=6MPa.

In this study, the interfacial tension between two phases is computed using the Weinaug-Katz equation (Eq. 1) before the drainage. More accurate results of interfacial tension may be considered by use of the density gradient theory [13]. Figs. 3-5 present $p_c$-$S_w$ curves of various miscible fluids calculated from our pore-network model with 4000 pore bodies. It is found that all of binary miscible fluids present the monotonous decrease in capillary pressure when the vapor-phase pressure $p^V$ increases from 2 MPa to 6 MPa. This phenomenon is dominant by the variation of interfacial tension. We can observe that the binary miscible fluids ($N_2$-$nC_4$, $C_1$-$nC_4$, and $CO_2$-$nC_4$) have similar $p_c$-$S_w$ curves at $p^V$=2 MPa, as shown in Fig. 3a. Differences among these miscible fluids on capillary behavoirs expand significantly as $p^V$ increases (see Figs. 3b and 3c). In addition, at the same $T$ and $p^V$ conditions, $N_2$, $C_1$, and $CO_2$ exhibit a higher capillary pressure when mixed with alkane with the longer carbon chain, as shown in Figs. 3a, 4a and 5a.

ICCS Camera Ready Version 2024
To cite this paper please use the final published version:
DOI: 10.1007/978-3-031-63783-4_1

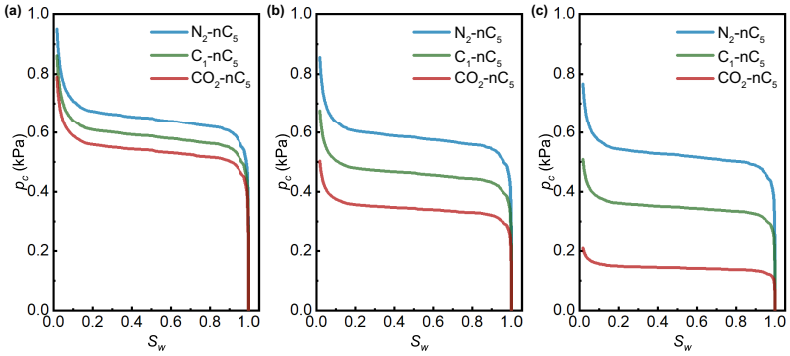


**Fig. 4.** The capillary behaviors of $N_2$-$nC_5$, $C_1$-$nC_5$, and $CO_2$-$nC_5$ miscible fluids at $T$=323K: (a) $p^V$=2MPa, (b) $p^V$=4MPa, and (c) $p^V$=6MPa.

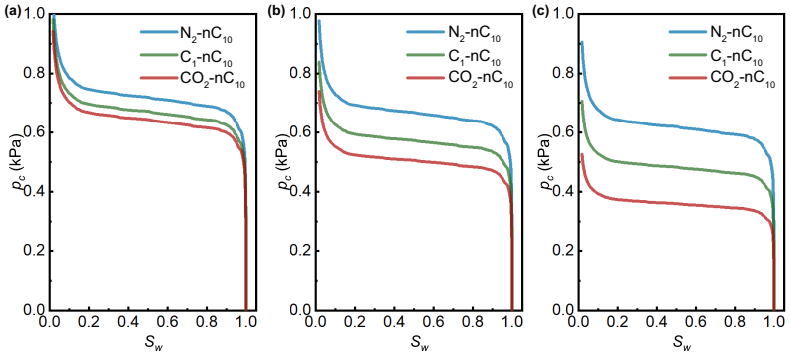


**Fig. 5.** The capillary behaviors of $N_2$-$nC_{10}$, $C_1$-$nC_{10}$, and $CO_2$-$nC_{10}$ miscible fluids at $T$=323K: (a) $p^V$=2MPa, (b) $p^V$=4MPa, and (c) $p^V$=6MPa.

Interfacial tension-induced capillary behaviors are very common in miscible fluids. Therefore, the estimation of these complex capillary behaviors using traditional pore-network modeling with the fixed interfacial tension may lead to large errors. Preliminary results in Figs. 3-5 have indicated that the thermodynamic analysis on pore-network modeling is needed in the future for the explanation of interactions between flow properties and phase miscibility.

## 4 Conclusions

We have simulated capillary behaviors of miscible fluids in porous media during the primary drainage process through the pore-network modeling method. Random generator-based pore-network models were developed by mainly introducing the Halton sequence and the Delaunay triangulation. Multiple cases in this work have shown that our network generation is efficient and robust, approaching the probability distribution properties of porous media. We have examined the effect

ICCS Camera Ready Version 2024
To cite this paper please use the final published version:
DOI: 10.1007/978-3-031-63783-4_1

of representative network sizes on capillary behaviors for generated pore-network models. It was found that simulations employing a network of 4000 pore bodies could successfully generate representative $p_c$-$S_w$ curves in our cases. Our simulation results indicate that it is essential to account for the thermodynamic effect of fluids when modeling capillary behaviors for miscible fluids.

**Acknowledgments.** This study is supported by King Abdullah University of Science and Technology (KAUST) through the grants BAS/1/1351-01 and URF/1/5028-01.

**Disclosure of Interests.** The authors have no competing interests to declare that are relevant to the content of this article.

## References

1. Li, Y., Yang, H., Sun, S.: Fully implicit two-phase VT-flash compositional flow simulation enhanced by multilayer nonlinear elimination. J. Comput. Phys. **449**, 110790 (2022)
2. Chen, S., Qin, C., Guo, B.: Fully implicit dynamic pore-network modeling of two-phase flow and phase change in porous media. Water Resour. Res. **56**(11), e2020WR028510 (2020)
3. Cardona, A., Liu, Q., Santamarina, J.C.: The capillary pressure vs. saturation curve for a fractured rock mass: fracture and matrix contributions. Sci. Rep. **13**(1), 12044 (2023)
4. Cui, R., Hassanizadeh, S.M., Sun, S.: Pore-network modeling of flow in shale nanopores: Network structure, flow principles, and computational algorithms. Earth-Sci. Rev. **234**, 104203 (2022)
5. Firoozabadi, A.: Thermodynamics and applications in hydrocarbon energy production. 1st edn. McGraw-Hill Education, New York, the United States (2016)
6. Kocis, L., Whiten, W.J.: Computational investigations of low-discrepancy sequences. ACM Trans. Math. Softw. **23**(2), 266–294 (1997)
7. Qin, C., Hassanizadeh, S.M., Ebigbo, A.: Pore-scale network modeling of microbially induced calcium carbonate precipitation: Insight into scale dependence of biogeochemical reaction rates. Water Resour. Res. **52**(11), 8794–8810 (2016)
8. Raoof, A., Hassanizadeh, S. M.: A new method for generating pore-network models of porous media. Transp. Porous Med. **81**, 391–407 (2010)
9. Joekar-Niasar, V., Hassanizadeh, S., Leijnse, A.: Insights into the relationships among capillary pressure, saturation, interfacial area and relative permeability using pore-network modeling. Transp. Porous Med. **74**, 201–219 (2008)
10. Cui, R., Feng, Q., Chen, H., Zhang, W., Wang, S.: Multiscale random pore network modeling of oil-water two-phase slip flow in shale matrix. J. Petrol. Sci. Eng. **175**, 46–59 (2019)
11. Joekar-Niasar, V., Hassanizadeh, S.M., Dahle, H.K.: Non-equilibrium effects in capillarity and interfacial area in two-phase flow: dynamic pore-network modelling. J. Fluid Mech. **655**, 38–71 (2010)
12. Li, Y., Kou, J., Sun, S.: Thermodynamically stable two-phase equilibrium calculation of hydrocarbon mixtures with capillary pressure. Ind. Eng. Chem. Res. **57**(50), 17276–17288 (2018)
13. Cui, R., Narayanan Nair, A.K., Che Ruslan, M.F.A., Yang, Y., Sun, S.: Interfacial properties of the hexane+ carbon dioxide+ brine system in the presence of hydrophilic silica. Ind. Eng. Chem. Res. **62**(34), 13470–13478 (2023)

ICCS Camera Ready Version 2024
To cite this paper please use the final published version:
DOI: 10.1007/978-3-031-63783-4_1